

HIGH-SPIN STRUCTURES OF THE NEAR-SPHERICAL NUCLEI $^{91,92}\text{Zr}$

P.C. SRIVASTAVA

Department of Physics, Indian Institute of Technology Roorkee
Roorkee, Uttarakhand 247667, India
pcsrifph@iitr.ac.in

(Received December 27, 2016; accepted May 18, 2017)

In the present work, we have interpreted recently available experimental data for high-spin states of the near-spherical nuclei $^{91,92}\text{Zr}$, using the shell-model calculations within the full $f_{5/2}, p_{3/2}, p_{1/2}, g_{9/2}$ model space for protons and valence neutrons in $g_{9/2}, g_{7/2}, d_{5/2}$ orbits. We have employed a truncation for the neutrons due to huge matrix dimensions, by allowing one neutron excitation from $g_{9/2}$ orbital to $d_{5/2}$ and $g_{7/2}$ orbitals. Results are in a good agreement with the available experimental data. Thus, theoretically, we have identified the structure of many high-spin states, which were tentatively assigned in the recent experimental work. The ^{91}Zr $21/2^+$ isomer lies at low-energy region due to fully aligned spins of two $g_{9/2}$ protons and one $d_{5/2}$ neutron.

DOI:10.5506/APhysPolB.48.807

1. Introduction

The nuclei around $N = 50$ region have recently attracted considerable experimental and theoretical attention [1–23]. The excitation of one neutron from $g_{9/2}$ to $d_{5/2}$ orbital is responsible for high-spin level structure of As, Sr, Y, Zr, Mo, Tc, Ru and Rh nuclei, with $N \sim 50$ [14, 24–34]. The importance of monopole fitted effective interaction, inclusion of higher orbitals across $N = 50$ shell and seniority quantum number are discussed in Refs. [35–39].

Recently, high-spin level structure of the semi-magic nucleus ^{91}Nb has been investigated via $^{82}\text{Se}(^{14}\text{N}, 5n)^{91}\text{Nb}$ reaction [18]. The importance of neutron particle-hole excitation across $N = 50$ shell gap is reported to describe the states above $\sim (21/2)\hbar$. The high-spin level structures of near-spherical nuclei $^{91,92}\text{Zr}$ have been reported in [7]. As we move from ^{91}Zr to ^{92}Zr , a possible reduction in the energy gap between $p_{3/2}$ and $p_{1/2}$ orbitals indicated, since one more neutron is excited across the $N = 50$ gap. For

^{92}Zr , Werner *et al.* [40] reported the pure neutron configuration to the 2_1^+ state, while the second excited quadrupole state shows the signatures of the one-phonon mixed-symmetric 2^+ state. The results of an in-beam study of high-spin structure of $^{94,95}\text{Mo}$ at GASP, Legnaro was reported in [41]. In this work, the authors also reported on shell-model results in $\pi(p_{1/2}, g_{9/2}, d_{5/2})$ and $\nu(p_{1/2}, g_{9/2}, g_{7/2}, d_{5/2}, d_{3/2}, s_{1/2})$ space. With this space, the yrast states 12_1^+ and 15_1^- in ^{94}Mo and those up to $25/2_1^+$ and $31/2_1^-$ in ^{95}Mo are explained. The importance of possible contribution from the $Z = 38$, $N = 50$ core, especially that of neutron excitations from the $g_{9/2}$ orbital, has been reported in this work.

In the present paper, we report on a systematic study of shell-model results for $^{91,92}\text{Zr}$. The aim of present work is to explain the structure of recently available high-spin experimental data for these two isotopes [7].

The work is organized as follows: details of the calculation and effective interaction are given in Section 2, the shell-model results and a comprehensive comparison with experimental data and wave-function analysis are given in Section 3. Finally, concluding remarks are drawn in Section 4.

2. Details about effective interaction

In this work, the results of recently available experimental data of $^{91,92}\text{Zr}$ have been interpreted with large scale shell-model calculations. The model space consists of full $f_{5/2}$, $p_{3/2}$, $p_{1/2}$, $g_{9/2}$ orbitals for protons and valence neutrons in $p_{1/2}$, $g_{9/2}$, $g_{7/2}$, $d_{5/2}$ orbitals. Since the dimension of matrices are very large, we allowed neutrons to occupy only $g_{9/2}$, $d_{5/2}$, $g_{7/2}$ orbitals. In the present work, we have taken ^{68}Ni as a core. We have allowed one neutron excitation from $g_{9/2}$ orbital to $d_{5/2}$ and $g_{7/2}$ orbitals. The calculations have been carried out with GWBXXG effective interaction. The single-particle energies (in MeV) for protons orbital are $f_{5/2} = -5.322$, $p_{3/2} = -6.144$, $p_{1/2} = -3.941$, $g_{9/2} = -1.250$, and for neutrons orbital are $g_{9/2} = -2.597$, $g_{7/2} = +5.159$, $d_{5/2} = +1.830$. We have performed shell model-calculation with shell-model code NuShellX [42]. The GWBXXG effective interaction is constructed with different interactions. The original 974 two-body matrix elements (TBMEs) were taken from bare G-matrix of H7B potential [43]. The bare G-matrix is not reasonable because of the space truncation and the interaction should be renormalized by taking into account the core-polarization effects. Here, the present G-matrix effective interaction is further tuned by modifying matrix elements with fitted interactions in the following way. The 65 TBMEs for proton orbitals were replaced with the effective values of Ji and Wildenthal [44]. The TBMEs connecting the $\pi(p_{1/2}, g_{9/2})$ and the $\nu(d_{5/2}, s_{1/2})$ orbitals were replaced by those from the work of Gloeckner [45], and those between the $\pi(p_{1/2}, g_{9/2})$

and the $\nu(p_{1/2}, g_{9/2})$ orbitals with those of Serduke *et al.* [46]. Previously, shell-model results with this interaction for the positive-parity yrast states of the neutron-rich ^{89}Rb , ^{92}Y , and ^{93}Y nuclei were reported in Ref. [47].

3. Results and discussions

3.1. Structure of ^{91}Zr

Results for energy levels of ^{91}Zr are shown in Fig. 1. The energy levels of positive parity states $5/2^+ - 33/2^+$ are compared with the available experimental data. The overall agreement with experimental data is good. The calculated $7/2_1^+$ is 282 keV below, while $9/2_1^+$ is 139 keV above the experimental data. In the case of negative parity, the calculation predicts a flip of levels for $11/2_1^-$ and $13/2_1^-$. The experimentally observed plausible state ($13/2_1^-$) at 2765 keV was predicted at 2924 keV. The calculated $35/2_1^-$ state is 181 keV lower than the experimental value. The ground state $5/2_1^+$ of ^{91}Zr is showing single-particle character with $\nu d_{5/2}$ configuration. The $7/2_1^+$ state has $\nu g_{7/2}$ configuration. The states $9/2_1^+ - 11/2_1^+ - 13/2_1^+ - 15/2_1^+ - 17/2_1^+ - 19/2_1^+ - 21/2_1^+$ mainly come from $\pi(f_{5/2}^6 p_{3/2}^4 g_{9/2}^2) \otimes \nu(d_{5/2}^1)$ con-

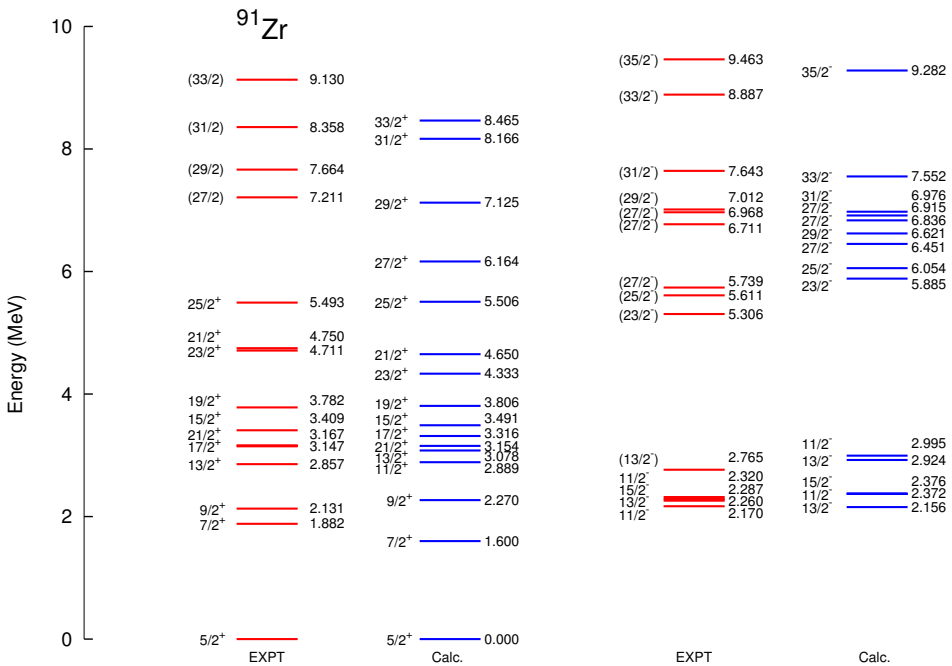


Fig. 1. Comparison of shell-model results for positive and negative parity states with experimental data for ^{91}Zr .

figuration. The low-lying isomeric $21/2_1^+$ state is formed with the fully aligned spin of two $g_{9/2}$ protons and one $d_{5/2}$ neutron. The positive-parity states beyond the $21/2_1^+$ isomer can be understood with different configuration as the proton excitations across the $Z = 38$ subshell and one neutron excitation from $\nu d_{5/2}$ to $\nu g_{7/2}$ orbital. The structure of $25/2_1^+$ and $27/2_1^+$ states come from $\pi(f_{5/2}^5 p_{3/2}^4 p_{1/2}^1 g_{9/2}^2) \otimes \nu(d_{5/2}^1)$ configuration. The $29/2_1^+$ state has $\pi(f_{5/2}^5 p_{3/2}^4 p_{1/2}^1 g_{9/2}^2) \otimes \nu(g_{7/2}^1)$ configuration. From $29/2_1^+$ to $31/2_1^+$, proton empties from $p_{1/2}$ to $g_{9/2}$ and configuration for $31/2_1^+$ becomes $\pi(f_{5/2}^4 p_{3/2}^4 g_{9/2}^4) \otimes \nu(g_{7/2}^1)$. The states $27/2_1^- - 29/2_1^- - 31/2_1^-$ come from $\pi(f_{5/2}^5 p_{3/2}^4 g_{9/2}^3) \otimes \nu(d_{5/2}^1)$, while $33/2_1^-$ has the $\pi(f_{5/2}^5 p_{3/2}^4 g_{9/2}^3) \otimes \nu(g_{7/2}^1)$ configuration. The $27/2_2^-$ state at 6711 keV has the $\pi(f_{5/2}^5 p_{3/2}^4 g_{9/2}^3) \otimes \nu(g_{7/2}^1)$ configuration.

The analysis of wave functions also helps us to identify which type of either proton or neutron pairs is broken to obtain the total angular momentum of the calculated states. The wave functions are decomposed in terms of the proton and neutron angular momenta I_p and I_n . These components are coupled to give the total angular momentum of each state. In Fig. 2, we have shown results of positive and negative parity states of ^{91}Zr . The positive parity states $19/2_1^+ - 21/2_1^+$ come from $I_p = 8^+ \otimes I_n = 5/2^+$. The dominant components are 84% ($19/2_1^+$), 92% ($21/2_1^+$). The $23/2_1^+$ comes from $I_p = 8^+ \otimes I_n = 7/2^+$ (90%), while for $25/2^+$, the configuration is $I_p = 10^+$

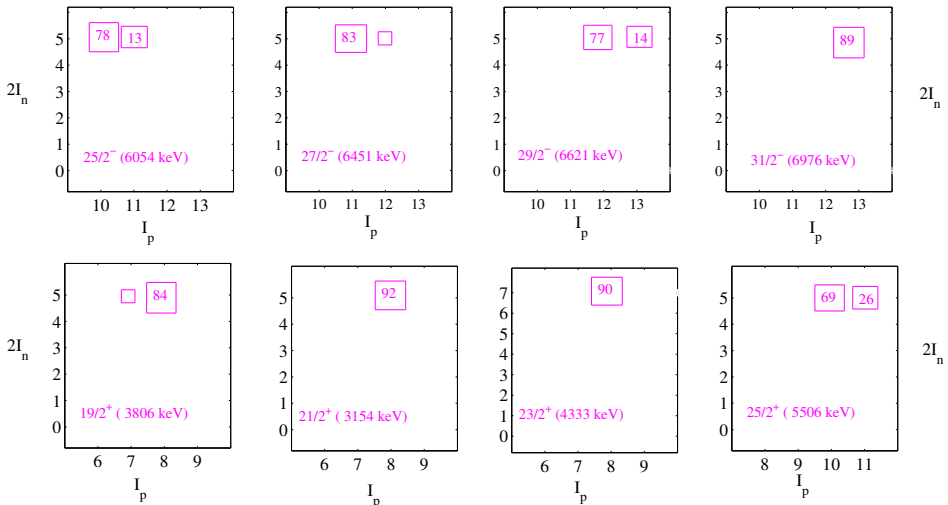


Fig. 2. Decomposition of the total angular momentum of selected states of ^{91}Zr into their $I_n \otimes I_p$ components. The percentage above 10% are written inside the squares, drawn with an area proportional to it. Percentage below 5% are not written.

$\otimes I_n = 5/2^+$ (69%) and $I_p = 11^+ \otimes I_n = 5/2^+$ (26%). Decomposition of the total angular momenta for the negative parity states $25/2_1^- - 31/2_1^-$ are also shown in Fig. 2. The $31/2_1^-$ state comes from $I_p = 13^- \otimes I_n = 5/2^+$ (89%). The experimental high-spin states (27/2), (29/2), (31/2) and (33/2) at 7211.4, 7663.7, 8358.2, 9129.8 keV, respectively, are plotted in Fig. 1. Although it is not possible to confirm from the shell model whether they are positive or negative parity states, nevertheless we have plotted the corresponding positive parity states predicted by shell model at 6164, 7125, 8166, 8465 keV, respectively. The configuration of $27/2_1^+$ is $I_p = 11^+ \otimes I_n = 5/2^+$ (94.4%); $29/2_1^+$ is $I_p = 11^+ \otimes I_n = 7/2^+$ (94.3%); $31/2_1^+$ is $I_p = 12^+ \otimes I_n = 7/2^+$ (79%); $33/2_1^+$ is $I_p = 8^+ \otimes I_n = 17/2^+$ (41%). The configuration for $33/2_1^+$ is $\pi(f_{5/2}^6 p_{3/2}^4 g_{9/2}^2) \otimes \nu(g_{9/2}^{-1} g_{7/2}^1 d_{5/2}^1)$. The $15/2_1^-$ at 2287.8 keV has an isomeric state, the shell-model calculation predicting it at 2376 keV, the configuration of this state is $\pi(f_{5/2}^6 p_{3/2}^4 p_{1/2}^1 g_{9/2}^1) \otimes \nu(d_{5/2}^1)$. This configuration is responsible for predicting $11/2_1^- - 13/2_1^- - 15/2_1^-$ states. The next negative parity $17/2_1^-$ state is coming from the $\pi(f_{5/2}^5 p_{3/2}^4 p_{1/2}^2 g_{9/2}^1) \otimes \nu(d_{5/2}^1)$ configuration.

3.2. Structure of ^{92}Zr

The results of ^{92}Zr are shown in Fig. 3. The dominant configuration of 0_1^+ , 2_1^+ , and 4_1^+ states is $\nu(d_{5/2}^2)$. The 6_1^+ and 8_1^+ states are at a large gap of 1.5 MeV from 4_1^+ state because we need more energy to excite protons from $p_{1/2}^2$ to $g_{9/2}^2$ orbital to form these two states ($[\pi g_{9/2}^2]_{6+,8+}$). The higher angular momentum states 10_1^+ and 12_1^+ are associated with $\pi g_{9/2}^2 \otimes \nu d_{5/2}^2$ configuration. Beyond 12_1^+ , other high-spin states arise from excitation of one proton/neutron across the $Z = 38/N = 56$ shell, *i.e.* one proton excitation from $(f_{5/2} p_{1/2}) \rightarrow g_{9/2}$ and one neutron from $d_{5/2} \rightarrow g_{7/2}$. The shell-model calculations predict first three 14^+ states at 4618, 6591, and 7063 keV, respectively. The 14^+ state at 6591 keV is due to $\pi(f_{5/2}^6 p_{3/2}^4 g_{9/2}^2) \otimes \nu(d_{5/2}^1 g_{7/2}^1)$ configuration. After looking at the structure and occupancy of three eigenvalues of calculated 14^+ states, we found that 12^+ (4728 keV) and 14^+ (6591 keV) have the same occupancy of $g_{7/2}$ and $d_{5/2}$ orbitals [also $B(E2)$ value for this transition is large]. Thus, we have taken 14^+ state at 6591 keV and 14^+ state at 7063 keV in Fig. 3 for the comparison with the experimental data. The structure of 14^+ state at 7063 keV is changed from 14^+ state at 6591 keV and it becomes $\pi(f_{5/2}^5 p_{3/2}^4 p_{1/2}^1 g_{9/2}^2) \otimes \nu(d_{5/2}^1 g_{7/2}^1)$. The average occupancy of $d_{5/2}$ orbital for 12^+ (5314 keV) and 14^+ (4618 keV) states is ~ 1.09 , while for 14^+ (7063 keV) state it is 1.83. This is also reflected from the structure change from 14^+ at 6591 keV to 14^+ at 7063 keV. The present study predicts that the 15_1^+ and 17_1^+ are

fully neutron-aligned states of the $\pi(f_{5/2}^5 p_{3/2}^4 p_{1/2}^1 g_{9/2}^2) \otimes \nu(d_{5/2}^1 g_{7/2}^1)$ configuration. These states are built on $I_n = 6^+$ [$\nu(d_{5/2}^1 g_{7/2}^1)$]. The negative parity state 5_1^- comes from $\pi(f_{5/2}^6 p_{3/2}^4 p_{1/2}^1 g_{9/2}^1)$ configuration and the 7_1^- to 9_1^- states from $\pi(f_{5/2}^6 p_{3/2}^4 p_{1/2}^1 g_{9/2}^1) \otimes \nu(d_{5/2}^2)$. The high-spin isomer 17_1^- observed in ^{92}Zr is reported at 8.041 MeV [48]; we have calculated this state at 7.781 MeV. The main component of the wave function of this state is $\pi(f_{5/2}^5 p_{3/2}^4 g_{9/2}^3) \otimes \nu(d_{5/2}^1 g_{7/2}^1)$.

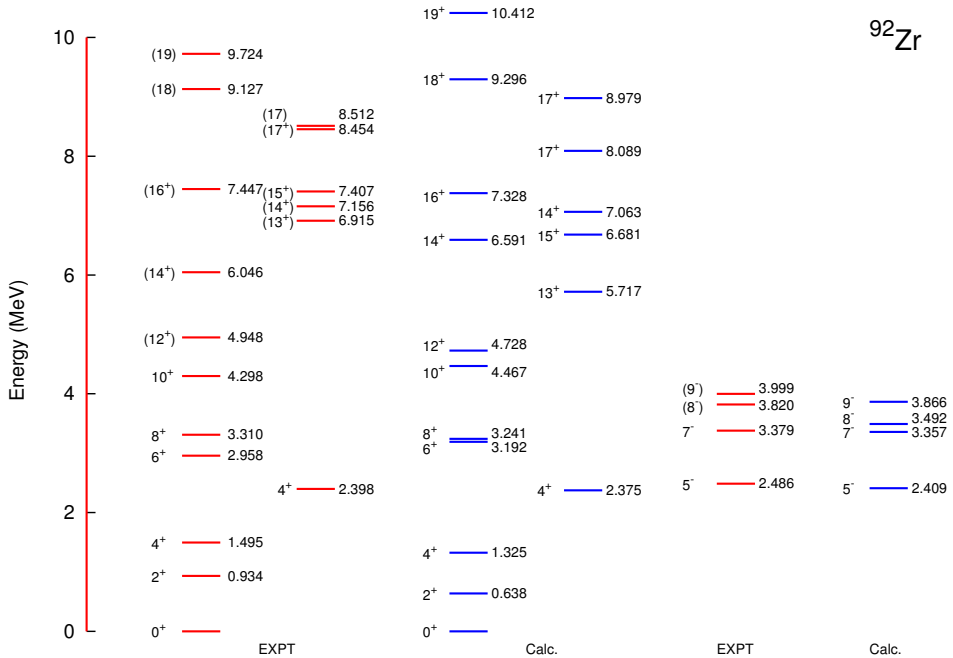


Fig. 3. Comparison of shell-model results for positive and negative parity states with experimental data for ^{92}Zr .

The wave function analysis for ^{92}Zr is shown in Fig. 4. The 14^+ (6591 keV) comes from $I_p = 8^+ \otimes I_n = 6^+$ (87%); the 14^+ (6591 keV) comes from $I_p = 8^+ \otimes I_n = 6^+$ (69%); 15^+ comes from $I_p = 9^+ - 10^+ \otimes I_n = 6^+$; 16_1^+ comes from $I_p = 10^+ - 11^+ \otimes I_n = 6^+$ and 17_1^+ comes from $I_p = 11^+ \otimes I_n = 6^+$ (94%). The composition of negative parity state 5_1^- comes from $I_p = 5^-$ (64%) configuration. The 7_1^- comes from, $I_p = 5^- \otimes I_n = 2^+$ (82%) and $I_p = 3_1^- \otimes I_n = 4^+$ (11%). The 8^- comes from $I_p = 4^- - 5^- \otimes I_n = 4^+$ (82%), while 9_1^- comes from $I_p = 5^- \otimes I_n = 4^+$ (95%). The experimentally observed high-spin plausible positive parity states (18) and (19) at 9129.6, 9724.2 keV are predicted by shell model at 9296, 10412 keV,

respectively. The configuration of 18_1^+ is $I_p = 12^+ \otimes I_n = 6^+$ (77%). For 19_1^+ , the major configuration is $I_p = 14^+ \otimes I_n = 6^+$ (52%) and another dominant configuration is $I_p = 13^+ \otimes I_n = 6^+$ (35%).

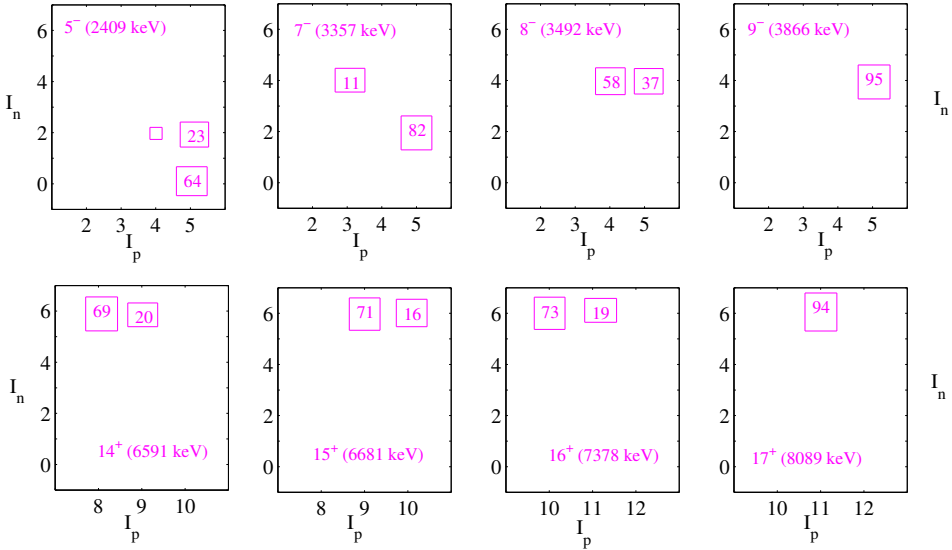


Fig. 4. Decomposition of the total angular momentum of selected states of ^{92}Zr into their $I_n \otimes I_p$ components. The percentage above 10% are written inside the squares, drawn with an area proportional to it. Percentage below 5% are not written.

There are two ways of generating high-spin angular momentum due to single-particle effects. First is by pair-breaking and second is due to particle-hole excitations. Thus, creating one-hole ($g_{9/2}^{-1}$) configuration is important for generating high-spin states.

The calculated energy levels of low-lying states for ^{92}Zr are more compressed. Thus, we have also performed second calculation (Calc. II) for ^{91}Zr and ^{92}Zr without neutron excitation from $\nu g_{9/2}$ to $\nu d_{5/2}$ orbital, *i.e.* we have completely filled the $\nu g_{9/2}$ orbital. The results are shown in Fig. 5. In the case of ^{92}Zr , the results for low-lying states $6_1^+ - 8_1^+ - 10_1^+ - 12_1^+$ show a good agreement with the experimental data. Previously, shell-model results for ^{92}Zr with the same effective interaction (TBMEs) for the proton ($p_{1/2}$, $g_{9/2}$) and neutron ($d_{5/2}$, $s_{1/2}$) orbitals were reported in Ref. [45]. The low-lying states in this restricted model space show a good agreement with the experimental data, although, high-spin states are not in good agreement without neutron excitation from $\nu g_{9/2}$ to $\nu d_{5/2}$ orbital, as we have shown in Figs. 1 and 3. The second set of calculations predicts 6_1^+ and 6_2^+ at 3355 and 3944 keV, respectively. Thus, reported 6^+ state is the first state.

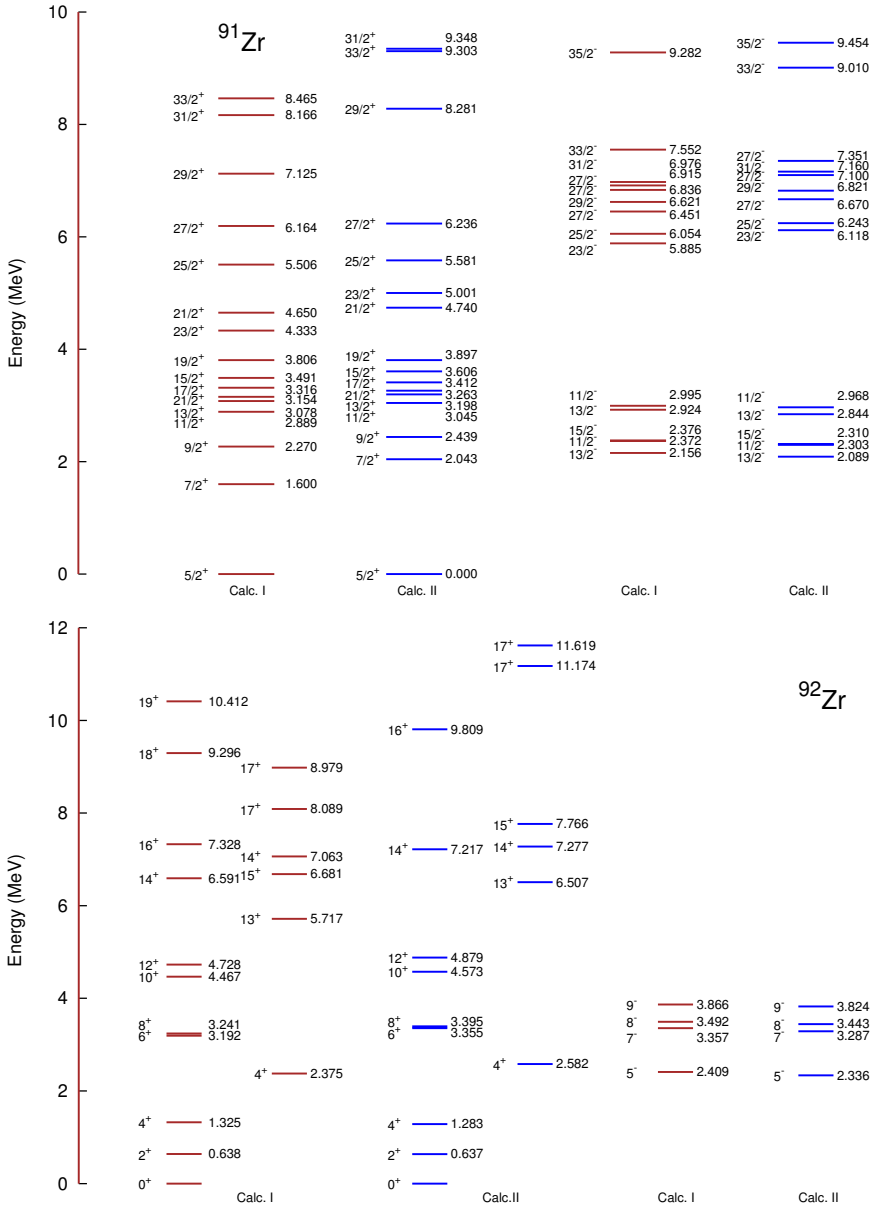


Fig. 5. Comparison of two different shell-model results for positive and negative parity states for ^{91}Zr and ^{92}Zr . First calculation with one neutron excitation from $g_{9/2}$ orbital to $d_{5/2}$ and $g_{7/2}$ orbitals (Calc. I) and second calculation with completely filled $\nu g_{9/2}$ orbital (Calc. II).

3.3. Electromagnetic properties

To test further the quality of our SM wave functions, we have calculated several E2 transitions which are listed in Table I. First, we have performed the calculations with the standard effective charges, *i.e.*, $e_\pi = 1.5e$ and $e_\nu = 0.5e$. Since the calculation without truncation is not feasible in the present model space, thus to account for the missing mixing of configurations, we have also performed calculations with the increased effective charges $e_\pi = 1.8e$ and $e_\nu = 0.8e$. This might be due to missing neutron orbitals below $p_{1/2}$, thus effect of core polarization is important. It also gives an explanation to adjust the effective charges such that the ground state transition strength is correctly reproduced as in the experimental data [1, 2, 40]. In Table I, we have listed both results. These results indicate deviation from experimental data even with the enhanced values of effective charges.

TABLE I

Experimental [49] and calculated $B(\text{E}2)$ values in W.u. with different sets of effective charges and $B(\text{M}1)$ with $g_s^{\text{eff}} = g_s^{\text{free}}$ (Set I)/ $g_s^{\text{eff}} = 0.7g_s^{\text{free}}$ (Set II).

Nucleus	Transition	Expt.	Set I		Set II	
			$e_\pi = 1.5e,$ $e_\nu = 0.5e$	$e_\pi = 1.8e$ $e_\nu = 0.8e$		
^{91}Zr	$B(\text{E}2; 7/2_1^+ \rightarrow 5/2_1^+)$	7.5(13)	1.44	2.34		
	$B(\text{E}2; 9/2_1^+ \rightarrow 5/2_1^+)$	4.2(6)	3.32	4.90		
	$B(\text{E}2; 13/2_1^+ \rightarrow 9/2_1^+)$	> 0.0079	6.31	9.51		
	$B(\text{E}2; 21/2_1^+ \rightarrow 17/2_1^+)$	4.3(7)	1.72	2.58		
^{92}Zr	$B(\text{E}2; 2_1^+ \rightarrow 0_1^+)$	6.4(6)	4.67	7.94		
	$B(\text{E}2; 4_1^+ \rightarrow 2_1^+)$	4.05(12)	1.97	3.69		
	$B(\text{E}2; 8_1^+ \rightarrow 6_1^+)$	3.59(22)	1.18	1.85		
	$B(\text{E}2; 12_1^+ \rightarrow 10_1^+)$	≥ 0.056	2.56	4.49		
	$B(\text{E}2; 14_2^+ \rightarrow 12_1^+)$		0.029	0.047		
	$B(\text{M}1; 2_2^+ \rightarrow 2_1^+)$	0.46(15)	0.164	0.117		

The calculated $B(\text{E}2; 8_1^+ \rightarrow 6_1^+)$ values with two sets of effective charges are small in comparison to the experimental data. In Table II, we have listed quadrupole and magnetic moments for the ground state and for few excited states. The results are in a good agreement with the experimental data for ^{91}Zr . From Table II, it is also possible to compare the recently available experimental data for the magnetic moments with the calculated values. The experimental value for $\mu(2_1^+)$ is $-0.360(20)$, while corresponding calculated value is -0.458 ($g_s^{\text{eff}} = 0.7g_s^{\text{free}}$). For 2_2^+ state, the experimental value for

$\mu(2_2^+)$ is $+1.5(10)$, while the corresponding calculated value is $+0.972$ ($g_s^{\text{eff}} = 0.7 g_s^{\text{free}}$). Similarly, for 4_1^+ state, the experimental value for $\mu(4_1^+)$ is $-2.0(4)$, while the corresponding calculated value is -1.456 ($g_s^{\text{eff}} = 0.7 g_s^{\text{free}}$).

TABLE II

Comparison of the calculated and the experimental [49] quadrupole (eb) and magnetic (μ_N^2) moments. The calculated quadrupole moment with $e_\pi = 1.5e$, $e_\nu = 0.5e$ (Set I)/ $e_\pi = 1.8e$, $e_\nu = 0.8e$ (Set II) and magnetic moment with $g_s^{\text{eff}} = g_s^{\text{free}}$ (Set I)/ $g_s^{\text{eff}} = 0.7 g_s^{\text{free}}$ (Set II).

	J^π	$Q_{s,\text{exp}}$	$Q_{s,\text{Set I}}$	$Q_{s,\text{Set II}}$	μ_{exp}	$\mu_{\text{Set I}}$	$\mu_{\text{Set II}}$
^{91}Zr	$5/2_1^+$	$-0.176(3)$	-0.203	-0.273	$-1.30362(2)$	-1.310	-0.900
^{92}Zr	2_1^+	N/A	$+0.158$	$+0.209$	$-0.360(20)$	-0.745	-0.458
	2_2^+	N/A	$+0.248$	$+0.319$	$+1.5(10)$	$+0.962$	$+0.972$
	4_1^+	N/A	-0.095	-0.136	$-2.0(4)$	-2.122	-1.456
	4_2^+	N/A	$+0.359$	$+0.448$	N/A	$+2.614$	$+2.498$

4. Conclusions

Structures of high-spin levels of $^{91,92}\text{Zr}$ have been studied with large-basis shell-model calculations with neutrons excitation across $N = 50$ shell. Following broad conclusions can be drawn from the present work:

- The present study reveals the importance of inclusion of $d_{5/2}$ and $g_{7/2}$ orbitals in the model space for high-spin states beyond ~ 4.5 MeV.
- The present shell-model results are in a good agreement with the proposed configurations in Ref. [7]. The structure of $25/2_1^+$ in ^{91}Zr is mainly from the $\pi(f_{5/2}^5 p_{3/2}^4 p_{1/2}^1 g_{9/2}^2) \otimes \nu d_{5/2}^1$ configuration. The structure of $27/2_1^- - 27/2_1^- - 31/2_1^-$ states come from $\pi(f_{5/2}^5 p_{3/2}^4 g_{9/2}^3) \otimes \nu d_{5/2}^1$ configuration, while $33/2_1^-$ have $\pi(f_{5/2}^5 p_{3/2}^4 g_{9/2}^3) \otimes \nu(g_{7/2}^1)$ configuration.
- For ^{92}Zr , 15_1^+ to 17_1^+ states are fully aligned states of the $\pi(f_{5/2}^5 p_{3/2}^4 p_{1/2}^1 g_{9/2}^2) \otimes \nu(d_{5/2}^1 g_{7/2}^1)$ configuration.
- We have calculated electromagnetic properties between different transitions for few high-spin states, wherever experimental data is available. These results indicate deviation with experimental data even with the enhanced values of effective charges.

I would like to acknowledge financial support from the faculty initiation grant. Thanks are due to Y.H. Zhang and Y.H. Qiang for useful suggestions during this work. I would like to thank Mirshod Ermamatov and V.K.B. Kota for a careful reading of the manuscript.

REFERENCES

- [1] J.D. Holt *et al.*, *Phys. Rev. C* **76**, 034325 (2007).
- [2] J.N. Orce *et al.*, *Phys. Rev. Lett.* **97**, 062504 (2006).
- [3] C. Fransen *et al.*, *Phys. Rev. C* **71**, 054304 (2005).
- [4] J.N. Orce *et al.*, *Phys. Rev. C* **82**, 044317 (2010).
- [5] P.H. Regan *et al.*, *AIP Conf. Proc.* **819**, 35 (2006).
- [6] A.D. Ayangeakaa, Master Thesis “Gamma-ray Spectroscopy of Shell Model States in $^{91,92}\text{Zr}$ ”, University of Surrey, 2006.
- [7] Z.G. Wang *et al.*, *Phys. Rev. C* **89**, 044308 (2014).
- [8] M. Honma, T. Otsuka, T. Mizusaki, M. Hjorth-Jensen, *Phys. Rev. C* **80**, 064323 (2009).
- [9] N. Yoshinaga, K. Higashiyama, P.H. Regan, *Phys. Rev. C* **78**, 044320 (2008).
- [10] H. Nakada, *Prog. Theor. Phys. (Kyoto), Suppl.* **196**, 371 (2012).
- [11] P.C. Srivastava, *J. Phys. G: Nucl. Part. Phys.* **39**, 015102 (2012).
- [12] P.C. Srivastava, *Mod. Phys. Lett. A* **27**, 1250061 (2012).
- [13] P.C. Srivastava, R. Sahu, V.K.B. Kota, *Eur. Phys. J. A* **51**, 3 (2015).
- [14] E. Sahin *et al.*, *Nucl. Phys. A* **893**, 1 (2012).
- [15] S. Saha *et al.*, *Phys. Rev. C* **86**, 034315 (2012).
- [16] S. Saha *et al.*, *Phys. Rev. C* **89**, 044315 (2014).
- [17] P. Singh *et al.*, *Phys. Rev. C* **90**, 014306 (2014).
- [18] P.W. Luo *et al.*, *Phys. Rev. C* **89**, 034318 (2014).
- [19] P. Federman, S. Pittel, *Phys. Lett. B* **69**, 385 (1977).
- [20] N.S. Pattabiraman *et al.*, *Phys. Rev. C* **65**, 044324 (2002).
- [21] M. Varga Pajtler *et al.*, *Nucl. Phys. A* **941**, 273 (2015).
- [22] C.R. Bingham, M.L. Halbert, *Phys. Rev. C* **2**, 2297 (1970).
- [23] P.C. Srivastava, V. Kumar, M.J. Ermamatov, *Acta. Phys. Pol. B* **47**, 2151 (2016).
- [24] M.-G. Porquet *et al.*, *Phys. Rev. C* **84**, 054305 (2011).
- [25] E. A. Stefanova *et al.*, *Nucl. Phys. A* **669**, 14 (2000).
- [26] E.A. Stefanova *et al.*, *Phys. Rev. C* **62**, 054314 (2000).
- [27] J. Reif *et al.*, *Nucl. Phys. A* **587**, 449 (1995).
- [28] E.K. Warburton *et al.*, *Phys. Rev. C* **31**, 1184 (1985).
- [29] N.S. Pattabiraman *et al.*, *Phys. Rev. C* **65**, 044324 (2002).

- [30] S.S. Ghugre, S.K. Datta, *Phys. Rev. C* **52**, 1881 (1995).
- [31] I.P. Johnstone, L.D. Skouras, *Phys. Rev. C* **55**, 1227 (1997).
- [32] H.A. Roth *et al.*, *Phys. Rev. C* **50**, 1330 (1994).
- [33] K. Sieja, F. Nowacki, K. Langanke, G. Martínez-Pinedo, *Phys. Rev. C* **79**, 064310 (2009).
- [34] P. Federman, S. Pittel, *Phys. Rev. C* **20**, 820 (1979).
- [35] R.K. Bansal, J.B. French, *Phys. Lett.* **11**, 145 (1964).
- [36] T. Otsuka *et al.*, *Phys. Rev. Lett.* **87**, 082502 (2001).
- [37] T. Otsuka *et al.*, *Phys. Rev. Lett.* **95**, 232502 (2005).
- [38] T. Faestermann, M. Górska, H. Grawe, *Prog. Part. Nucl. Phys.* **69**, 85 (2013).
- [39] I. Talmi, *Simple Models of Complex Nuclei*, Harwood Academic Publishers, Switzerland, 1993.
- [40] V. Werner *et al.*, *Phys. Lett. B* **550**, 140 (2002).
- [41] Y.H. Zhang *et al.*, *Phys. Rev. C* **79**, 044316 (2009).
- [42] B.A. Brown, W.D.M. Rae, E. McDonald, M. Horoi, NuShellX@MSU.
- [43] A. Hosaka, K.-I. Kubo, H. Toki, *Nucl. Phys. A* **444**, 76 (1985).
- [44] X. Ji, B.H. Wildenthal, *Phys. Rev. C* **37**, 1256 (1988).
- [45] D.H. Gloeckner, *Nucl. Phys. A* **253**, 301 (1975).
- [46] F.J.D. Serduke, R.D. Lawson, D.H. Gloeckner, *Nucl. Phys. A* **256**, 45 (1976).
- [47] D. Bucurescu *et al.*, *Phys. Rev. C* **76**, 064301 (2007).
- [48] G. Korschinek *et al.*, Proceedings of the International Conference on Nuclear Structure, Tokyo, 1977.
- [49] C.M. Baglin, *Nucl. Data Sheets* **113**, 2187 (2012).